Computation Studies of Air Flow in Two Dimensional Coaxial Pipe

Adi Surjosatyo and
Farid Nasir Ani

Fakulti Kejuruteraan Mekanikal
Universiti Teknologi Malaysia
81310 UTM Skudai, Johor DT, Malaysia

Abstract: The present study conducted a computer simulation of a turbulent flow in a two co-axial pipes with varying pipe diameter and entrance displacement (ΔL). The entrained flow characteristics together with the effect of the temperature of the entrance flow inlet were studied with variation of ΔL. The numerical method employs differencing scheme for integrating the continuity equation and energy equation. An equation k-ε turbulent model was used to simulate the turbulent transport quantities. A Fluent CFD modeling package was used to produce 2-D predictions of the flow pattern. Results show that increasing the air entrained temperature until 600 K will decrease the air flow rate and the diameter ratio of 2.81 has the highest entrained flowrate.

Key words: *Coaxial pipes, k-ε turbulent model, CFD modeling, 2D flow, entrance displacement, air ejector.*

INTRODUCTION

Ejectors are apparatus which entrained the low pressure gas by high pressure gas interchanging the momentum of high speed driving gas discharged through a nozzle (or nozzles) with momentum of low pressure entrained gas around the driving jet (or jets). Ejectors usually consists of a nozzle (or nozzles) and a diffuser. That is, it have no moving part such as a rotor or piston. One of the merits of ejector is that it is simple in construction and it could compressed a large flow rate of driving gas for the small and simple size ejector design as shown on Figure 1.

There are other names for the system which have the same working principles, such as jet pump, injector and eductor. The general name for these system is jet apparatus. The names above mentioned are distinguished according to the kinds, states and properties such as compressibility (gas, liquid, mixture of liquid and solid, mixture of gas, liquid and solid) of the driving and entrained fluids. Based on the normal ejector design the present study is to propose some data for the design of the subsonic air in a coaxial pipe configuration.

A research on ejector by Johannesen (1951) reported that the features of ejector driven by and entraining compressible fluids. These include the aerodynamics of flow in the actuating

nozzle, mixing chamber and the supersonic and subsonic diffusers. In general, the emphasis are made on the steam driven air ejector and experiments were made on such ejectors covering a range of geometrical proportions and pressure ratios.

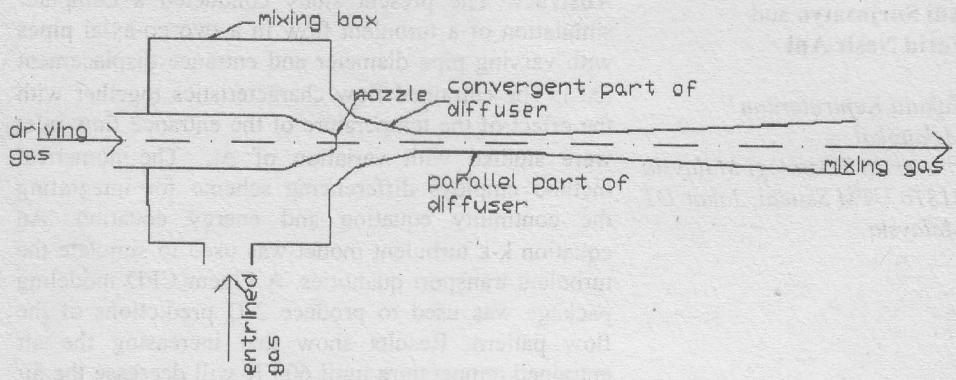

Figure 1. Ejector configuration

A one dimensional method of analysis of air ejector is presented by Keenan et al. (1950). The analysis considers mixing of the primary and secondary streams at constant pressure and constant area and it is concluded that better performance will result from constant-pressure mixing. It should be noted, however, that while experimental verification of the analysis constant area is good, the lack of a suitable design of constant-pressure mixing chamber has prevented from demonstrating the calculated supremacy of this ejector design.

There are many of the previous paper deal with single and multiple nozzle ejector. In the implementation of these design should have a high air compression ($\geq$ 2 bars) to have a sufficient entrained air. In the present work it will be developed by another type of a simple ejector in the form a pair of coaxial pipe which has a purpose to work on low air compression ($\leq$ 2 bars). The present study is objected to so-called an ejector which deals with compressible gases as the driving gas and entrained gas. One of the merits is that it could use a blower with low power and entrained gas could occur which matches a specially fixed application.

THE AIR EJECTOR MODEL

Figure 2 shows the air flow and configuration of the coaxial pipes. The primary air or driving air is introduced into the inlet pipe I which acts as nozzle function. It is to be expected due to pressure drop at outlet pipe I occur the entrained air flow in pipe II which acts as diffuser function.

In this model the length of driving pipe or pipe I is 665 mm and the length of entrain ejector pipe is 650 mm. The pipe entrance displacement start from from ΔL=50 mm (0.050 m) and it increased until ΔL= 420 mm (0.420 m). Diameter Ratio (DR) means here the diameter ratio of entrain ejector pipe to the drive pipe. The different size of entrain ejector diameter are varied while the drive pipe diameter is constant. The Diameter Ratio (DR) variation are 1.63, 2.34, 2.62 and 2.81. In this model is assumed that there is no friction on the surface pipe. Therefore the calculation regarding to the wall roughness is negligible.

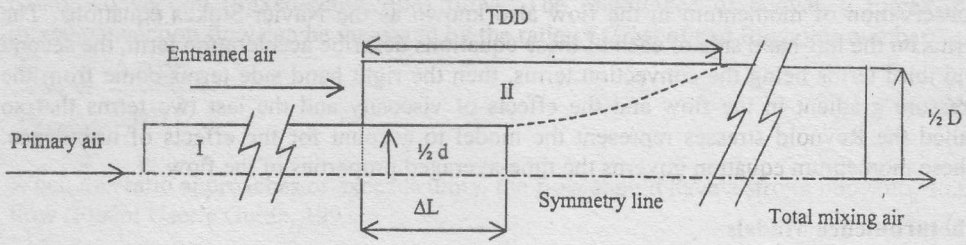

I : driving pipe; ΔL : pipe entrance displacement; TDD : Touch down distance
II : entrained pipe; D,d : entrain and drive pipe diameters; DR: Diameter Ratio (D/d)

Figure 2. Air flow and ejector - drive pipes

GOVERNING EQUATIONS

The physical model considered in this work are shown schematically in Figure 2. This configuration is a two dimensional of co-axial pipe with turbulent flow in the two pipes. The governing Reynolds-averaged equations for steady-state turbulent flow of two-dimensional (Fluent User's Guide, 1997; Shaw, 1998; Patankar, 1980) are as followed:

Continuity Equations:

a. incompressible fluid:

$$\frac{\partial U}{\partial X}+\frac{\partial V}{\partial Y}=0 \qquad (1)$$

b. compressible fluid:

$$\frac{\partial \rho}{\partial t}+\frac{\partial(\rho U)}{\partial X}+\frac{\partial(\rho V)}{\partial Y}=0 \qquad (2)$$

Momentum Equations:

a.

$$\rho\frac{\partial U}{\partial t}+\rho U\frac{\partial U}{\partial X}+\rho V\frac{\partial U}{\partial Y}=-\frac{\partial P}{\partial X}+\frac{\partial}{\partial X}(\nu\frac{\partial U}{\partial X})+\frac{\partial}{\partial Y}(\nu\frac{\partial U}{\partial Y})+$$

$$\frac{\partial}{\partial X}(-\overline{u'u'})+\frac{\partial}{\partial Y}(-\overline{u'v'}) \qquad (3)$$

b.
$$\rho\frac{\partial V}{\partial t}+\rho V\frac{\partial V}{\partial X}+\rho V\frac{\partial V}{\partial Y}=-\frac{\partial P}{\partial Y}+\frac{\partial}{\partial X}(\nu\frac{\partial V}{\partial X})+\frac{\partial}{\partial Y}(\nu\frac{\partial V}{\partial Y})+$$
$$\frac{\partial}{\partial X}(-\overline{u'v'})+\frac{\partial}{\partial Y}(-\overline{v'v'}) \quad (4)$$

The two equations, Eq. (3) and (4) derived from Newton's Second Law, describe the conservation of momentum in the flow also known as the Navier-Stokes equations. The terms on the left-hand side of each of these equations describe acceleration term, the second and third terms being the convection terms, then the right hand side terms come from the pressure gradient in the flow and the effects of viscosity and the last two terms that so called the Reynold stresses represent the model to account for the effects of turbulence. These momentum equation governs the time-averaged properties of the flow.

Theturbulence Models

To solve Equations (1) to (4), a turbulence model for the turbulent transport quantities has to be specified. In the present work, the standard k-ε model (Fluent User's Guide, 1997; Shaw, 1998; Launder and Spalding, 1972) based on Boussineq hypothesis is adopted. The local mean state of turbulence can be characterized by the turbulent kinetik energy k and its dissipation rate ε according to:

$$\rho\,\overline{u_i'u_j'}=\rho\frac{2}{3}k\delta_{ij}-\nu(\frac{\partial u_i}{\partial x_j}+\frac{\partial u_j}{\partial x_i})+\frac{2}{3}\nu\frac{\partial u_i}{\partial X_i}\delta_{ij} \quad (5)$$

where

$$k = \frac{1}{2}\sum_i \overline{u_i'^2} \quad (6)$$

$$\nu = \rho C_{\upsilon l}\frac{k^2}{\varepsilon} \quad (7)$$

$$\varepsilon = k^{2/3}/l_\varepsilon \quad (8)$$

Transport Equation For K And ε

The values of k and ε Equation (7) are obtained by solution of conservation energy:

$$\frac{\partial}{\partial t}(\rho k)+\frac{\partial}{\partial X_i}(\rho u_i k)=\frac{\partial}{\partial X_i}(\frac{\upsilon}{\sigma_k}\frac{\partial k}{\partial X_i})+G_k+G_b-\rho\varepsilon \quad (9)$$

$$\frac{\partial}{\partial t}(\rho\varepsilon)+\frac{\partial}{\partial X_i}(\rho u_i\varepsilon)=\frac{\partial}{\partial X_i}(\frac{\upsilon}{\sigma_\varepsilon}\frac{\partial\varepsilon}{\partial X_i})+C_{1\varepsilon}\frac{\varepsilon}{k}(G_k+(1-C_{3\varepsilon})G_b)-C_{2\varepsilon}\rho\frac{\varepsilon^2}{k} \quad (10)$$

where

$$G_k=\upsilon(\frac{\partial u_j}{\partial X_i}+\frac{\partial u_i}{\partial X_j})\frac{\partial u_j}{\partial x_j} \quad (11)$$

$$G_b = -g_i \frac{\upsilon}{\rho \sigma_h} \frac{\partial \rho}{\partial X_i} \quad (12)$$

The Effects of Turbulence on Heat Transfer

When the heat is added to a fluid and the fluid density with temperature flow can be induced due to the force of gravity acting on the density variations. Such flows are termed natural-convection (mixed-convection) flows. The importance of buoyancy forces in a mixed convection flow can be measured by the ratio of Grashof and Reynolds number:

$$\frac{G_r}{R_e} = \frac{\Delta \rho g h_c}{\rho \upsilon^2} \quad (13)$$

When this ratio approaches or exceeds unity, the flow should have a strong buoyancy to the flow (Fluent User's Guide, 1997).

In this simulation, there are some correlation between the turbulence flow and the fluid flow temperature. This correlation is based on the momentum equation and again the Boussineq model is adopted. For simplifying the momentum equation, it will perform the flow in y-direction (Shaw, 1989):

$$\frac{\partial V}{\partial t} + U\frac{\partial V}{\partial X} + V\frac{\partial V}{\partial Y} = -\frac{1}{\rho}\frac{\partial p}{\partial Y} + \frac{\mu}{\rho}\left(\frac{\partial^2 V}{\partial X^2} + \frac{\partial^2 V}{\partial Y^2}\right) + g\beta(T - T_f) \quad (14)$$

Another theoretical correlation is based on the conservation of energy which can predicted the heat transfer process within the fluid and/or within solid in the model (Fluent User's Guide, 1997). The simulation model solve the energy equation in the form of a transport equation for the static enthalpy, h:

$$\frac{\partial}{\partial t}(\rho h) + \frac{\partial}{\partial X_i}(\rho u_i h) = \frac{\partial}{\partial X_i}\left(k_c + k_t \frac{\partial T}{\partial X_i}\right) - \frac{\partial}{\partial X_i}\sum_j h_j J_j + \frac{\partial p}{\partial t} + \tau_{ik}\frac{\partial U_i}{\partial X_k} + S_h \quad . \quad (15)$$

Enthalpy h defined as:

$$h = \sum_j m\, h_j \quad (16)$$

where: $h_j = \int_{T_{ref}}^{T} c_{p,j}\, dT$

NUMERICAL METHOD

The commercial software package, Fluent version 4.4, produced by Fluent Inc. was used as the primary source code for the model. This package employs a control volume-based, finite difference solution technique to allow full characterization of the flow field. The Reynolds-averaged Navier-Stokes equations coupled with the Reynolds-averaged

governing differential equations of continuity, energy, and species are solved in a discritized form. The standard k-ε turbulence modelis employed. To obtain values at control volume interfaces needed for flux calculations, the power law interpolation scheme is utilised. The pressure-linked continuity and momentum equations are solved using the Semi-Implicit Method for Pressure-Linked Equations Consistent (SIMPLEC) solution algorithm. Specific details regarding convergence parameters such as multi-grid and under relaxation factors are available in Fluent. The convergence criterion is specified as the relative difference of every dependent variable between iteration steps being smaller than 10^{-6}. The pipe form in the present work is assumed as circular form.

CONDITIONS OF SIMULATION

Simulations of subsonic air ejector was done according to obtain an optimum condition of air flowrate in a pair of coaxial pipe. The simulations are being carried out using a CFD software package. The conditions of simulation are as follows:

- subsonic and compressible air flow
- turbulence method: k- ε method
- boundary conditions:
  i) inlet pressure as primary air at inside-pipe: 2 bars,
  ii) inlet pressure where the secondary air or entrance air is induced: 1 bar (atmospheric pressure),
  iii) inlet pressure at the outlet pipe where the exit of total air flow takes place: 1 bar (atmospheric pressure),
- 2 D flow analysing.

RESULTS AND DISCUSSIONS

Effect of Variation of Diameter Ratio on Air Velocity and Air Flowrate

Figure 3 to Figure 4 show the graphs of air velocity (AV) and air flowrate (AF) versus diameter ratio. Each of the Figures has two types of curve, namely, primary (driving air) and entrained air flow. For primary air flow is kept constant. The displacement of entrance pipe has not much influence to the primary air flowrate curve due to the pressure intake is high enough compared to the pipe resistance, but for the entrained air flow there is a reduce both for air velocity and flowrate. The increasing of pipe displacement means increasing of flow path. Therefore the area of entrained air flow is more restricted. It means the flow path for the entrained air has more resistance. From the graph that the highest entrained air flow is achieved at 0.05 m where this distance is on the first drive pipe displacement.

Figure 5 and 6 show the effect Diameter Ratio variation on entrained air flowrate. Figure 5 plotted curves in which the increasing of DR has caused the entrained mass flowrate also increased.

To describing both of these conditions it is necessary the continuity equation is to be implemented:

$$\frac{\partial}{\partial t}\int \rho dv + \int \rho v.dA = 0 \qquad (17)$$

Assumed the flow is steady, therefore the first term is zero ($\frac{\partial}{\partial t}\int \rho dv = 0$), hence:

$$\int \rho v.dA = 0 \qquad (18)$$

Since there is no flow through the wall and the flow is compressible, the equation (18) changed into:

$$\rho_1 V_1 A_1 = \rho_2 V_2 A_2 = \dot{m} \qquad (19)$$

According to the Equation (19), when DR increase means the area of flow is also increase, so the volumetric flow rate $\dot{m}$ is also increase as in Figure 5 and air flow velocity is decreased as shown in Figure 6.

Effect of Diameter Ratio and Drive Pipe Displacement on Touch Down Distance (TDD)

Figure 7 and 8 show the graphs of the effect of both diameter ratio and drive pipe displacement (ΔL) on Touch Down Distance (TDD). In these graphs three curves were plotted. Diameter Ratio (DR) 1.63, 2.34 and 2.62 have created the touch down distance, except for the highest displacement ΔL 0.420 m. In this displacement there is no touch down point on the entrain pipe and it has created turbulence effect on the outlet section of the entrain pipe since TDD is beyond the length of the pipe. Consequently, this condition could cause a flow resistance. The TDD have a tend to increase for higher DR. Figure 7 show the smallest TDD is achieved by the smallest displacement. Also increasing the entrance displacement the TDD increased also as in Figure 8. It should be that there is a correlation between the entrained mass air flowrate and TDD. It means the entrained flow path, since it is affecting reduction of the mass air flowrate, influence the TDD significantly.

Graphs show that higher DR could influence higher entrained mass and increasing of this mass flowrate has affected TDD to increase flowrate as in Figure 7. Due to the DR variation has a correlation with flow area which has influenced mass air flowrate, thus it could be deducted the flow area is a factor which has also influenced TDD. Graphs on Figure 8 show that higher ΔL has increased TDD. It means that TDD is affected by air flow path between the drive pipe and entrain pipe.

Effect of Variation of Gas Temperature on Entrained Air Flowrate and Air Velocity

Figure 9 to Figure 12 show graphs of entrained air flowrate and air velocity at different ambient temperature of the inlet secondary pipe (entrance pipe). These figures show that the increasing of air temperatures of 300, 500 and 600 °C at different Diameter Ratio DR of 1.63, 2.34, 2.62 and 2.81 which have influenced the variation of air flowrate and velocity. The increasing of gas temperature affected the increasing the entrained air velocity, but there is a decreasing of entrained air flowrate.

The properties of air at atmospheric pressure (Holman, 1993) are listed in tables i.e. value of air density and specific heat which are correlated with different air temperature. Increasing of air temperature affect the decreasing of air density and increasing of specific heat. There is a correlation at the gas law (Streeter, 1983; Fluent User's Guide, 1997; Holman, 1993) between air density and the temperature as follow:

$$\rho = p_{op}/RT_a \qquad (20)$$

If the temperature increase, the air density should be decrease. Based on the continuity equation, namely, Equation 19 the decreasing of density affected the air flowrate, it means the air flowrate is decreased. Another explanation is based on energy equation as in Equation 16. Increasing the air temperature is effecting the increment of specific heat capasity value c_p (Cengel, 1999). To balancing the total heat capacity of the system the mass flowrate should decrease.

Increasing of the temperature effecting also the air velocity. When the system changes from some initial velocity v_1 to a velocity v_2, the corresponding change in kinetic energy is (Holman, 1993):

$$\Delta E = KE_2 - KE_1 = \int_{v_1}^{v_2} \frac{m}{g_c} v\, dv = \frac{1}{2g_c} m (v_2^2 - v_1^2) \qquad . (21)$$

The conservation energy shows that when the temperature in a system is increasing then the heat Q in the system increase also. It means there is a change in the internal energy ΔE. The work W is altered according to the conservation energy by the amount of heat energy added Q, thus:

$$Q + W = \Delta E \qquad . (22)$$

It indicates that
Energy added to system = accumulation of energy in the system.
At the present work there is no work W or W = 0, thus Equation 22 becomes

$$Q = \Delta E \qquad (23)$$

where $Q = h_i = \int_{T_{ref}}^{T} c_{p,i} dT$.

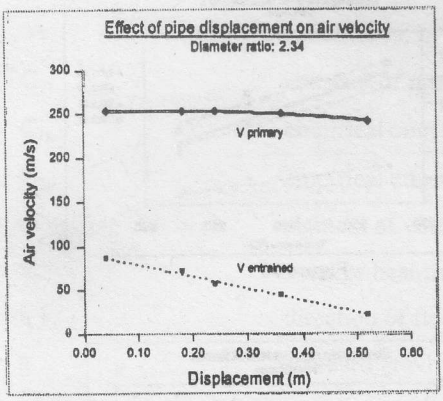

Figure 3

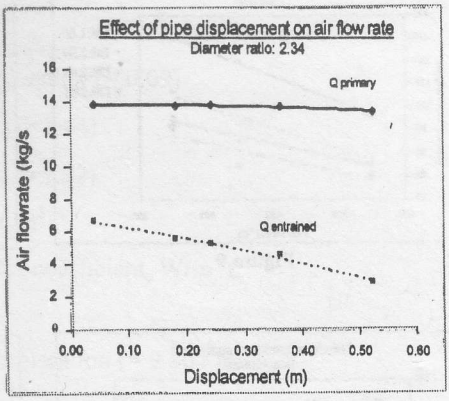

Figure 4

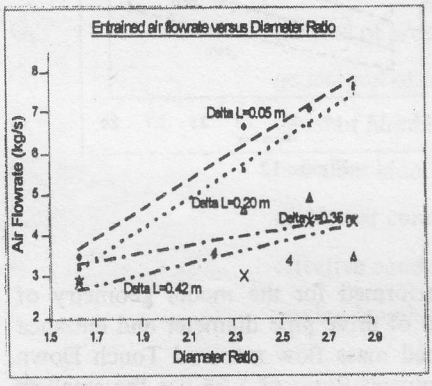

Figure 5

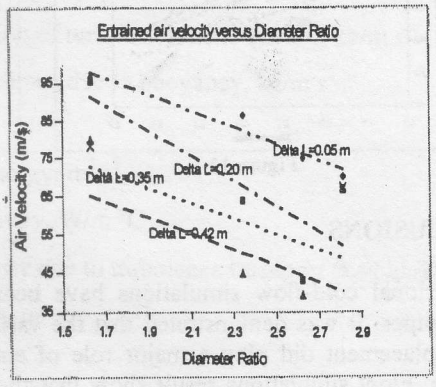

Figure 6

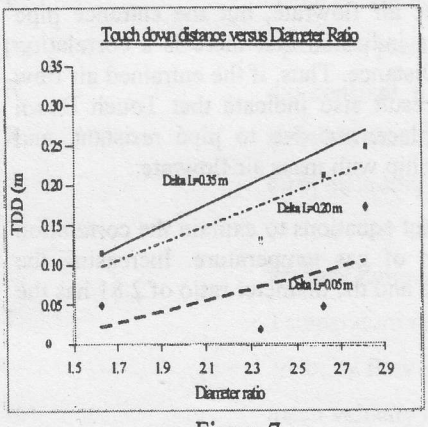

Figure 7

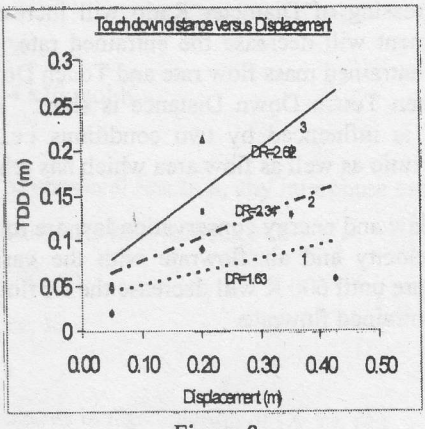

Figure 8

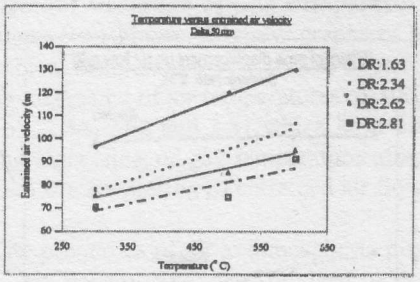

Figure 9

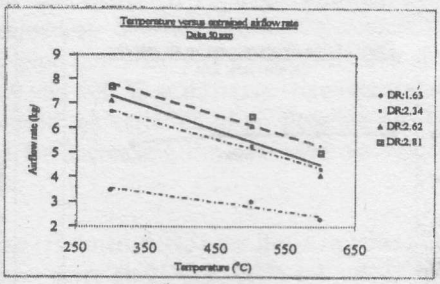

Figure 10

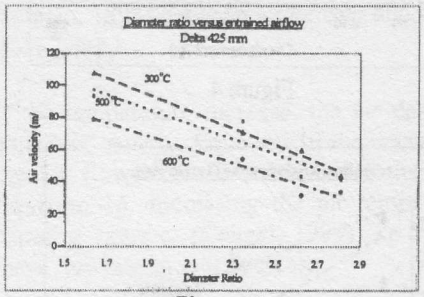

Figure 11

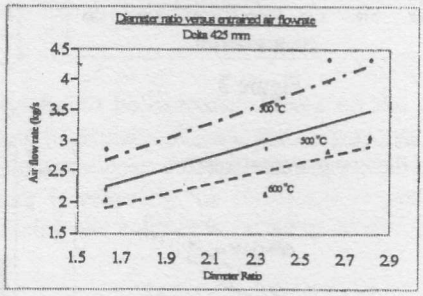

Figure 12

CONCLUSIONS

2-dimensional cold-flow simulations have been performed for the model geometry of coaxial pipes. It was demonstrated that the variation of drive pipe diameter and entrance pipe displacement did play a major role of entrained mass flow rate and Touch Down Distance. Flow simulations result show that the Diameter Ratio of 1.63 has the smallest flow area, as the consequence, there is the lowest entrained air flowrate. For each diameter ratio increasing of Diameter Ratio will increase the air flowrate, but the entrance pipe displacement will decrease the entrained rate. It has indicated that there is a correlation between entrained mass flow rate and Touch Down Distance. Thus, if the entrained air flow is low then Touch Down Distance is short. The result also indicate that Touch Down Distance is influenced by two conditions i.e., displacement due to pipe resistant, and diameter ratio as well as flow area which has relationship with mass air flowrate.

The gas law and energy conservation law are important equations to explain the correlation of air velocity and air flowrate with the variation of gas temperature. Increasing the temperature until 600 K will decrease the air flow rate and the diameter ratio of 2.81 has the highest entrained flowrate.

NOMENCLATURE

A	inflow area, m^2
C_{v1}	constant of proportionality (= 0.09)
$C_{1\varepsilon}$	empirical constants (=1.44)
$C_{2\varepsilon}$	empirical constants (=1.92)
dv	element of volume, m^3
h_c	average heat transfer coefficient, W/m °C
i, j	direction of flow, -
g	standard gravity acceleration (= 9.807 m/s^2)
$g\beta(T-T_f)$	additional term for buoyancy
J_j'	diffusion flux of the species j'
G_k	the rate of production of turbulent kinetic energy, kg/m s^3
G_b	generation of turbulence due to buoyancy, kg/m s^2
G_r	Grashof number
k	turbulent kinetic energy, m^2/s^2
k_c	molecular conductivity, W/m °C
k_t	effective conductivity due to turbulence transport ($k_t=c_p\mu_t/Pr_t$)
l_ε	mixing length scale, m
$\dot{m}$	volumetric flow rate, kg/s
P	mean pressure, Pa
p_{op}	operating pressure, Pa
R	gas constant, 8.31434 kJ/kmol K
R_e	Reynold number, -
S_h	term including heat of chemical reaction, any interphase exchange of heat, any other volumetric heat sources, -
T_a	ambient temperature, K
T_f	Temperature reference, K
t	velocity flow time, s
U,V	mean velocity components in the direction of (X,Y), m/s

v	inflow velocity, m/s
u',v'	fluctuating components velocity in the direction of (X,Y), m/s
β	coefficient of volume expansion, 1/K $= \frac{1}{v}(\frac{\partial v}{\partial T})_p = -\frac{1}{\rho}(\frac{\partial \rho}{\partial T})_p$
$\overline{u'u'}$	Reynold stresses, m^2/s^2
$\overline{u'v'}$	Reynold stresses, m^2/s^2
$\overline{v'v'}$	Reynold stresses, m^2/s^2
ρ	density, kg/m^3
δ_{ij}	wall shear layer thickness, m
σ_k	"Prandtl" numbers governing the turbulent diffusion of k and ε, (=1.0)
σ_ε	Prandt numbers governing the turbulent diffusion of k and ε, (=1.3)
μ	turbulent viscosity is proportional to the product of a turbulent velocity scale and length scale, $N.s/m^2$
υ	kinematik viscosity, m^2/s
ε	distribution of dissipation rate of k, m^2/s^3

ACKNOWLEDGMENT

The authors are grateful to RMC (Research Management Center), UTM for supporting the fund to this research.

LITERATURES

[1] Yamamoto, F., *Performance of Subsonic Air Ejector with multiple nozzles*, Memoires of The Faculty of Engineering, Fukui University, Vol. 30 No.1 1982.
[2] Streeter, V, L., *Fluid Mechanics*, McGraw-Hill International Book Company, 1983.
[3] Fluent User's Guide, *Fluent 4.4*, Vol. 1, 3 and 4, May 1997.
[4] Holman, J.P., *Thermodynamics*, McGraw-Hill International Book Company, 1993.

[5] Johannesen, N. H, *Ejector theory and experiments*, Danish Acad. Tech. Sci. No.1. 176pp (1951).
[6] Strahle, W.C., *Jannaf Thermochemical Table – An Introduction to Combustion*, 1993.
[7] Keenan, L. H., Neumann, E.P. and Lustwerk, F. P., *An investigation of ejector design by analysis and experiment* J. Appl. Mech., 17, 3 (1950).
[8] Shaw, C. T, *Computational Fluid Dynamic*, Longman, 1989.
[9] Panton, R. L., *Incompressible Flow*, John Willey & Sons, 1984.
[10] Patankar, S.V., *Numerical Heat Transfer and Fluid Flow*, Hemisphere Publishing Corporation, 1980.
[11] Launder, B. E., and Spalding, D.B., *Lectures in Mathematical Models of Turbulence*, Academic Press, London, England, 1972.
[12] Hwang, R. R. and Chow, Y. C., *Computation of turbulent flow over two-dimensional surface-mounted rib*, Proceedings of t he 6th Flow Modelling and Turbulence Measurements, Florida, 1996.
[13] Cengel, Yunus, *Heat Transfer: A Practical Approach,* McGraw Hill, 1998.